X-645-71-203
PREPRINT

NASA TM X- 65563

MAGNETOSPHERIC FIELD DISTORTIONS OBSERVED BY OGO's 3 and 5

N71-27604
(ACCESSION NUMBER)
(THRU)
44
(PAGES)
G3
(CODE)
TMX-65563
(NASA CR OR TMX OR AD NUMBER)
13
(CATEGORY)
FACILITY FORM 602

M. SUGIURA
B. G. LEDLEY
T. L. SKILLMAN
J. P. HEPPNER

MAY 1971

GSFC
GODDARD SPACE FLIGHT CENTER
GREENBELT, MARYLAND

Magnetospheric Field Distortions Observed by OGO's 3 and 5

M. Sugiura, B. G. Ledley, T. L. Skillman
and J. P. Heppner

May 1971

Laboratory for Space Physics
NASA-Goddard Space Flight Center
Greenbelt, Maryland 20771

ABSTRACT

Magnetospheric field distortions are studied using approximately 10,000 data points sampled from the rubidium magnetometer measurements on OGO's 3 and 5. Analysis is made in terms of ΔB defined as the observed field magnitude minus the magnitude of a reference geomagnetic field. Average contours of equal ΔB are shown in the geomagnetic noon-midnight and dawn-dusk meridian planes for magnetically quiet ($Kp = 0\text{-}1$) and slightly disturbed ($Kp = 2\text{-}3$) conditions. These ΔB contour maps show (a) a high latitude $+\Delta B$ region on the night side and (b) an equatorial $-\Delta B$ region in the inner magnetosphere. Regarding (a), the present survey, extending approximately to 60° N dipole latitude in the relevant area, indicates a region of maximum ΔB at $\gtrsim 60^{\circ}$ dipole latitude and at ~ 6 to $8\ R_e$ near geomagnetic midnight. Values of ΔB increase with increasing magnetic activity, and peak values exceed 50γ for $Kp = 2\text{-}3$. The existence of a region of such high ΔB cannot be accounted for by the existing models of the magnetosphere; it suggests that there is additional magnetic pressure on the polar cap magnetosphere. The high latitude $+\Delta B$ region extends toward the dayside magnetosphere beyond dawn and dusk with decreasing magnitude of ΔB. Though the observations presented here do not cover southern high latitudes at appropriate geocentric distances to directly detect a southern counterpart of the $+\Delta B$ region, there is no indication in the available data to suggest absence of a similar region in the southern hemisphere. Region (b), i.e., the equatorial $-\Delta B$ region encircling the earth, shows greater inflation of the inner magnetosphere during magnetically quiet periods than the inflation usually assumed. The average minimum ΔB between 2 and 5 R_e is approximately -40γ for quiet ($Kp = 0\text{-}1$) conditions

and -50γ for slightly disturbed ($Kp = 2-3$) conditions. The equatorial distribution of observed ΔB as a function of geocentric distance differs substantially from that expected from the well-known models of the quiet-time ring current. While the calculated model ring current field has a minimum near the center of the ring current belt and recovers appreciably before leveling off toward the earth, observed ΔB decreases toward the earth to distances $\lesssim 3\ R_e$ even at quiet times. The proton population observed by Frank near $6.5\ R_e$ is not directly associated with the quiet-time inflation of the inner magnetosphere discussed here. There must be a population of low-energy particles with substantial total energy near the equator at distances of 2 to 5 R_e that has not been definitively measured.

INTRODUCTION

Measurements of the magnetic field in the magnetosphere have been made on numerous satellites, and the gross features of the field distribution are known. Reviews of these observations have been given by Heppner (1967a, 1967b), Ness (1967, 1969), Fairfield (1970), Sugiura (1971) and others. In spite of the seemingly extensive observations the actual coverage of observation in the inner magnetosphere and in the polar regions is extremely limited, except at low altitudes where OGO's 2 and 4 (Cain and Langel, 1971) Cosmos 49 (Benkova and Dolginov, 1971) and 1964-83C (Zmuda, 1971) have surveyed the earth's main field extensively. This limitation in coverage stems largely from the fact that the data used in the past studies of the magnetospheric field distribution have been obtained by fluxgate magnetometers that had low saturation fields. The fluxgate magnetometer on Explorer 26 had a relatively wide range $\pm$ 2000 γ, but the published results of analysis of the data from that satellite mainly concerned storm time ring current effects (Cahill, 1966, 1970).

In the present paper the rubidium vapor magnetometer data of the scalar magnetic field intensity obtained by the OGO 3 and 5 satellites are analyzed to study the magnetospheric field distortions. The instrument, described by Ledley (1970), measured the field in the range 3 to 14,000 γ, the upper limit being imposed by the telemetry limitation. The primary purpose of this paper is to describe the magnetic field distortions in the magnetosphere in terms of the field magnitude under quiet and slightly disturbed conditions. Deviations from these average states during magnetospheric substorms and magnetic storms are not treated in this paper.

An analysis of the type discussed here was initially attempted with the OGO 1 fluxgate magnetometer, but only with limited results because of the malfunctioning of that satellite and the consequent difficulties in interpreting the measurements made (Heppner et al., 1967). Results of a preliminary study of the OGO 3 and 5 data were presented by Sugiura et al., (1970); the present paper greatly expands these earlier investigations. A future paper utilizing data being processed from the GSFC fluxgate magnetometer on OGO 5 will extend the analysis to vector differences for $B \leq 2000\ \gamma$.

SATELLITE ORBITS AND DATA ANALYSIS

OGO's 3 and 5 were launched on June 7, 1966 and March 4, 1968, respectively, with the following initial orbit parameters:

	Inclination	Geocentric Distances		Period
		Perigee	Apogee	
OGO 3	31.0°	1.05 R_e	20.17 R_e	48.6 hours
OGO 5	31.3	1.05	24.03	62.4

(1 Re = 1 earth radius)

The present study uses sampled rubidium magnetometer data taken by OGO 3 between June 9, 1966 and November 21, 1967, and by OGO 5 between April 7, 1968 and August 5, 1969. During these periods OGO 3 apogee completed approximately 1½ revolutions about the earth and OGO 5 apogee, approximately 1 1/3 revolutions. The data roughly cover all local times though not necessarily evenly due to data gaps and orbital factors.

For a magnetospheric field survey, sampling methods with fixed temporal or spatial intervals are generally not meaningful because of the highly variable rates of both the spatial gradient in the field and of the change in the satellite speed along the orbit. Hence, a flexible sampling technique was adopted. At large distances where the field gradient is small, as in the tail, data were sampled once in 20 to 30 minutes; with decreasing distance, the sampling frequency was increased. As a general rule, the sampling reaches the highest rate of once in 2 minutes when the satellite enters the high field region near the earth and the latitude of its position changes at a very rapid rate. Approximately 4,000 data points were sampled from OGO 3 and 6,000 from OGO 5. These sampled data are instantaneous values. The rubidium magnetometer signals were routinely reduced at a rate of 6.94 readings per second. Samples were selected for the present analysis only when they were representative of the values in their vicinity. This was assured by inspecting microfilmed data plots made at the rate of 2 minutes of data per frame. In fact, in most cases sampled data agreed within $\pm$ 1γ with the averages taken over 2 minute intervals centered at the sampled points. Had 2 minute averages been used instead of instantaneous values the results of the present analysis, which is mainly concerned with fields at distances $\gtrsim$ 3 R_e, would be identical.

In obtaining ΔB the reference field was calculated using the main field model of Jensen and Cain (1962) for OGO 3 and the GSFC (12/66) model of Cain et al., (1967) for OGO 5. Ideally, use of a more recent, common reference field for both satellites is desirable, but the present analysis is part of a continuing program begun shortly after launch of each satellite. In each case the respective reference field was selected as being the best representation of the main field at the time the computation of the satellite orbit was initiated. At the radial distances considered in this paper, differences between the main field models are not large enough to significantly modify the results. A provision has been made in the data analysis to recalculate ΔB by replacing the reference field if such a step is called for in future studies of the near earth field.

ΔB DISTRIBUTION

To describe main gross features of magnetospheric distortions, the following averaging and smoothing procedure was adopted. The magnetosphere was divided into quadrants centered at geomagnetic midnight, dawn (6 hr), noon, and dusk (18 hr). Each quadrant was further divided into volume elements with dipole latitude (θ) intervals of 5^{o} and radial distance (r) intervals of 1 R_e. Data in each of these volume elements were averaged and assigned to the center of the volume element. Thus, such averages were placed at network of points on the four meridian half-planes mentioned above. Smooth contour lines of equal ΔB were then drawn on each meridian half-plane. For simplicity, regions in which $\Delta B > 0$ are called $+\Delta B$ regions, and those in which $\Delta B < 0$, $-\Delta B$ regions; likewise, + signs in front of ΔB merely indicate sign of ΔB itself, and are not to be taken as algebratic expressions meaning ($\pm$ 1) ΔB.

(i) Quiet Conditions, Kp = 0-1

Figure 1 shows equal ΔB contours in the geomagnetic noon-midnight meridian plane based on data obtained during magnetically quiet periods as respresented by Kp = 0-1. A theoretical magnetopause and dipole field lines are drawn in merely to give a convenient frame of reference without any direct relation to the observed data. Contour lines are drawn at 10γ intervals, and broken lines indicate interpolated or extrapolated data. Blank areas at high latitudes (and those at lower latitudes in later figures) were not covered by the data used in the present analysis.

Near the magnetopause on the noon side, the low latitude $+\Delta B$ and the change-over to $-\Delta B$ at higher latitudes are consistent with the ΔB distribution expected from magnetopause currents in existing theoretical models (Figure 5). In other regions there are two important differences to observe. They are: (a) the large field depression in the equatorial region of the inner magnetosphere, and (b) the existence of a high $+\Delta B$ region toward the nightside polar magnetosphere. The magnitude of the equatorial $-\Delta B$ increases toward the innermost magnetosphere where $-\Delta B$ becomes less than -40γ.

Similar contours of equal ΔB in the geomagnetic dawn-dusk meridian plane, also for Kp = 0-1, are shown in Figure 2. The equatorial field depression in the inner magnetosphere and the high latitude $+\Delta B$ regions are evident. The maxima in ΔB in the latter regions are not as high as in the midnight sector.

(ii) Slightly Disturbed Conditions, Kp = 2-3

Figure 3 gives equal ΔB contours in the geomagnetic noon-midnight meridian plane for slightly disturbed conditions represented by Kp = 2-3. The general basic features are similar to those in Figure 1 for Kp = 0-1, except that $-\Delta B$ in the equatorial inner magnetosphere and $+\Delta B$ at high latitudes on the night side are both intensified compared with the corresponding values in Figure 1. For midnight, the equatorial $-\Delta B$ is below -50γ and the high latitude $+\Delta B$ exceeds 50γ.

Equal ΔB contours in the dawn-dusk meridian plane for Kp = 2-3 are presented in Figure 4. Here again the general features are similar to those in Figure 2 for Kp = 0-1 except that $\pm\ \Delta B$ have been intensified.

(iii) ΔB Contours for the Mead-Williams Model

To demonstrate that the regions of large $+\Delta B$ at high latitudes in the nightside magnetosphere cannot be accounted for by the neutral sheet current in the tail, ΔB contours for the magnetosphere model presented by Williams and Mead (1965) are shown in Figure 5. The tail field is intentionally made larger than the observed tail field in Figure 3 to see if there is any tendency for the model tail field to increase ΔB toward the polar magnetosphere. It is obvious from Figure 5 that there is no possibility of explaining the high latitude $+\Delta B$ with a tail current. It might be questioned whether or not inclusion of return currents on the tail magnetopause might alter this situation. An extensive study has been made on this point by using a model neutral sheet current that closes its circuit on the magnetopause, thereby assuring that the tail magnetic flux is nearly confined in the magnetosphere. Even with such a model it is not possible to produce the observed ΔB distribution. Since it is a negative result, the details of the model calculation are not discussed here.

(iv) Quiet-time Ring Current

To compare the distribution of the observed low latitude ΔB with that predicted from the quiet-time ring current of the type generally calculated, ΔB contours for a theoretical model are shown in Figure 6. The theoretical model was supplied by Hoffman and Berko (private communication) who calculated the ring current field by the technique developed by Hoffman and Bracken (1965, 1967). Since we are concerned with the general characteristics of ΔB deduced from the standard model ring current as compared with those of observed ΔB, we will not discuss the detailed specifics of the particle distribution used by Hoffman and Berko. For the present purpose it suffices to note that this model ring current field contains the main features common to models of Akasofu et al. (1962) and of Hoffman and Bracken (1965, 1967).

Topological characteristics of ΔB in the inner magnetosphere seen in Figure 6 are not similar to those in Figures 1 and 3; here the model calculation was made for a condition appropriate for noon. Differences are more clearly demonstrated in Figure 7, in which the equatorial ΔB is plotted against radial distance both for the theoretical model and for the observation. For the model ring current there is a large depression of the field near the center of a ring current belt, and the field recovers appreciably before leveling off toward the earth. In contrast, the curves for observed ΔB, shown for noon and midnight and for Kp = 0-1 and 2-3, continue to decrease toward the earth to distances less than 4 R_e. Thus the geometry of the quiet-time ring current must be more disk-shaped than doughnut-shaped, and it must extend inward to distances well below 4 R_e, and possibly below 3 R_e. Further discussions on the quiet-time ring current are given in a later section. It should also be noted that from the topological character of the high latitude $+\Delta B$ regions it appears implausible that ring current inflation of the inner magnetosphere can produce the high field regions.

(v) ΔB vs. Dipole Latitude

Examples of ΔB plots as a function of dipole latitude in the noon and midnight quandrants of a spherical shell at a given radial distance are presented in Figures 8 and 9. In these figures two such shells, 2 R_e thick and centered at geocentric distances 5 and 7 R_e, respectively, are taken. Before plotting ΔB, data were further sampled on each orbit so that intervals between any neighboring data points are not less than 1 R_e. Thus, in each of Figures 8 and 9 the maximum number of points contributing from any one orbit traversing the shell is two, so that points in these figures are highly independent. Different symbols are used to represent ΔB values for different levels of magnetic activity: namely, dots for Kp = 0-1, open circles for Kp = 2-3, and triangles for Kp $\geq$ 4.

In both Figures 8 and 9 the equatorial $-\Delta B$ region and the $+\Delta B$ regions at mid- to high latitudes in the northern and southern hemispheres are evident. Increasing $+\Delta B$ with increasing magnetic activity as represented by Kp is clearly indicated. Increasing magnitude of $-\Delta B$ with increasing activity in the equatorial region can also be seen in Figure 9. Black dots for Kp = 0-1 in Figures 8 and 9 show that near the noon-midnight meridian plane and at radial distances 4 to 8 R_e the variation of ΔB with dipole latitude is a remarkably stable feature, considering the long time span over which the observations were made.

Significance of field distortion as represented by ΔB can be very clearly understood when ΔB is shown in terms of the ratio $\Delta B/B_o$ where B_o is the magnitude of the reference field. Table 1 gives maximum values of $\Delta B/B_o$, as percentages, for the data used in Figures 8 and 9. Even under quiet conditions the maximum percentage for the $+\Delta B$ region was as high as 34% (Kp = 1) at 7.8 R_e and 20.8^o dipole latitude, and for the $-\Delta B$ region, 52% (Kp = 1) at 7.8 R_e and -2.8^o dipole latitude. The overall maximum percentage of $+\Delta B$ for the entire data set used in Figures 8 and 9 was 87%, recorded at 8.0 R_e and 25.7^o dipole latitude during a Kp = 7 interval.

Referring to Table 1, the maximum ratio, $\Delta B/B_o$, increases with increasing magnetic activity for the $+\Delta B$ regions, but the maximum ratio for the $-\Delta B$ regions does not follow this rule. This is because large field decreases tend to occur at closer distances to the earth as the intensity of disturbance increases.

Table 1. Maximum values of $\Delta B/B_o$, expressed in percentage, for the data used in Figures 8 and 9: $\pm$ signs for $\pm$ ΔB regions.

	4-6 Re	6-8 Re
Kp = 0-1	+ 18% - 20	+ 34% - 52
Kp = 2-3	+ 23 - 18	+ 43 - 38
Kp ≥ 4	+ 39 ——	+ 87 - 43

EQUATORIAL CROSSING DISTANCES OF FIELD LINES VS. DIPOLE LATITUDES OF THEIR FEET ON THE EARTH: NOON AND MIDNIGHT.

With the results obtained in this study it is possible to determine approximate relations between the dipole latitudes of the feet of field lines on the earth's surface and the radial distances of their equatorial crossing points in the noon-midnight meridian plane. This determination was made by equating (a) the radial component of magnetic flux crossing the earth's surface within a longitude (or local time) segment $d\phi$ centered at ϕ, here taken to be at noon or midnight, and between the dipole equator ($\theta = 0$) and latitude θ to (b) the θ component of the <u>same</u> flux crossing the dipole equatorial plane within $d\phi'$ at ϕ' and between the earth's surface (ρ=1) and radial distance ρ earth radii: that is, by the relation

$$-a^2\, d\phi \int_0^{\theta} B_r\, (\rho=1,\theta,\phi)\, \cos\theta d\theta = a^2\, d\phi' \int_1^{\rho} B_\theta\, (\rho,\theta=0,\phi')\, \rho d\rho$$

where a is the earth's radius and $\rho = r/a$.

In general, $\phi \neq \phi'$ and $d\phi \neq d\phi'$ because of the azimuthal bending of field lines. Fairfield (1968), in constructing his magnetospheric field model, used field vectors projected onto the solar magnetic equatorial plane to obtain the correspondence between ϕ and ϕ' and $d\phi$ and $d\phi'$. In the present calculation we assume that in the immediate vicinity of the noon-midnight meridian plane the azimuthal bending of field lines is negligible, and therefore that for noon or midnight, $\phi' = \phi$ and $d\phi' = d\phi$ in the limit $d\phi \to 0$. We further assume that on the dipole equatorial plane the field is perpendicular to this plane and hence that at the equator, $B_\theta = B_0 + \Delta B$, where B_0 is the magnitude of the dipole field. At the earth's surface B_r is also based on the dipole field.

Figure 10 shows the results of calculations made for noon and midnight for two levels of magnetic activity, Kp = 0-1 and 2-3; for comparison, the curve for the dipole field is also shown. The apparent changes in slopes at $\theta = 60^\circ$ are merely due to the use of different scales for θ above and below this latitude.

Based on Figure 10, for instance, the equatorial crossing distances for a field line leaving the earth at dipole latitude 64.6° (e.g., College, Alaska) are about 5.85 and 6.1 R_e respectively, at noon and midnight for Kp = 0-1; the corresponding distances for slightly disturbed conditions, Kp = 2-3, are about

5.7 R_e and 6.5 R_e, respectively. For comparison, the corresponding distance for the dipole field is 5.45 R_e. These are of course, average positions and significantly smaller or larger displacements can be expected in individual cases. According to Figure 3 of Fairfield's (1968) paper the approximate equatorial crossing distance for the same field line is roughly 5.3 R_e for noon and 5.5 R_e for midnight. The differences between the estimates from his model and those from ours are largely due to the fact that the inflation of the inner magnetosphere assumed by Fairfield on the basis of the then available material was considerably smaller than is found in the present analysis.

Estimates of equatorial crossing distances of field lines for greater disturbances are obviously of great interest, but such estimates will have to be deferred until analysis of highly disturbed conditions is completed.

Figure 10 indicates that for field lines up to about 70°, the equatorial crossing points move inward near noon and outward near midnight as magnetic activity increases (within the range of activity treated here). This behavior near noon means that the compression of the magnetosphere by the increased solar wind pressure has on the average a greater effect on these field lines than the expansion of the inner magnetosphere. The large effect of the solar wind compression can also be seen in Figure 7 by observing that ΔB is greater for Kp = 2-3 than for Kp = 0-1 beyond about 6.6 R_e for noon.

According to the present model the average dipole latitude of the foot of the field line passing through a synchronous satellite at 6.6 R_e would be 66.1° at noon and 65.3° at midnight when Kp = 0-1, and 66.5° at noon and 64.8° at midnight when Kp = 2-3. For the dipole field the corresponding latitude is 67°. Thus, the field lines near the synchronous orbit move in the radial direction appreciably during the course of the day even when the magnetosphere is relatively quiet.

There are obvious limitations in the technique used above because of asymmetry in the field distortion with respect to the dipole equator and of other simplifying assumptions made. Nevertheless, we believe that these results are the best one can hope for at the present stage of the analysis, and that they provide the most reliable data available at present.

DISCUSSIONS

(i) At the Synchronous Orbit

Because of the undetermined spacecraft fields the fluxgate magnetometer measurements on the synchronous satellites ATS 1 (Cummings and Coleman, 1968) and ATS 5 (Skillman, 1970) do not provide absolute values of the magnetospheric field components, in particular, the horizontal component, H. Observations of relative changes have, however, given valuable results. Based on the present statistical analysis, the equatorial ΔB for noon at 6.6 R_e is about 12γ for both Kp = 0-1 and 2-3. Since the dipole field on the equator at this distance is 108γ, the average noon value of H at the synchronous orbit is approximately 120γ for Kp = 0-3. At midnight, ΔB = -23γ for Kp = 0-1, and ΔB = -33γ for Kp = 2-3 at the same equatorial radial distance. Thus, the average midnight field magnitude at the synchronous orbit is approximately 85γ for Kp = 0-1 and 75γ for Kp = 2-3. The average daily amplitude in H is 35γ for Kp = 0-1 and 45γ for Kp = 2-3. Because of as yet inadequate coverage of equatorial regions near dawn and dusk the present analysis does not yield curves for average daily variations at the synchronous altitude. However, on the basis of the available data it is a reasonable assumption that the maximum occurs near noon and the minimum near midnight. Observations on ATS 1 and 5 agree with this assertion.

Cummings et al., (1968) used a zero level for H in which the average noon and midnight values were 135γ and 105γ, respectively. While the amplitude of 30γ can be considered as being in agreement with our result, their zero level was set too high by about 15γ. As they were concerned primarily with relative changes in the field, this offset is of no consequence to their discussions of magnetospheric substorms. However, their procedure of fitting the model of Williams and Mead (1965) to the observed average diurnal variation by suitably choosing several parameters in the model seems to be questionable.

More recently, Olson and Cummings (1970) compared the ATS 1 observations with the fields predicted by several magnetospheric models. They attributed the observed diurnal variation with an amplitude of 30 to 40γ (which, as it should be, is in good agreement with our results) to the combined effect of the magnetopause current and the neutral sheet current of the tail. However, the present results, for instance, Figures 1 to 4, indicate that the inflation of the inner magnetosphere plays the vital role in producing the diurnal variation at the synchronous orbit. This circumstance is also demonstrated by the fact that the zero level selected by Cummings et al., (1968) is too high; this is a factor that cannot be reconciled by adjusting parameters in the model used by these authors.

(ii) <u>Further Discussions on the Quiet-time Ring Current</u>

Following the Explorer 12 observations of protons with energies $\geq$ 100 kev by Davis and Williamson (1963), storm and quiet-time ring currents were calculated by several workers (Akasofu et al., 1962; Hoffman and Bracken, 1965, 1967). Frank (1967, 1970, 1971) has made extensive studies of the ring current using observations of low-energy protons and electrons ($\sim$200 ev to 50 kev) obtained on OGO 3. Frank (1967, 1971) and Frank and Owens (1970) associated a distribution of these low-energy protons centered at $\sim$ 6 to 7 R_e with the quiet-time ring current.

The results of the magnetic field observations on OGO's 3 and 5, however, do not give support to the location of the "quiet-time ring current" which Frank's observations appeared to identify. This is not a suggestion that Frank's observations are faulty. The results presented here simply imply that energy and pitch angle parameters have not both been adequately measured, and/or that the particle sampling has not provided adequate data close to the equatorial plane at 2-5 R_e. Our results indicate that a field depression of $\sim 40\gamma$ exists at such close distances as $\lesssim 3$ R_e when Kp = 0-1. This magnitude differs substantially from Frank's (1967) estimate of about -10γ for the field depression at the earth's surface caused by his quiet-time ring current. A similar estimate of -12γ was given by Hoffman and Bracken (1965) based on an assumed proton distribution which is consistent with the Explorer 12 observation by Davis and Williamson (1963). [Hoffman and Bracken have revised their figure of -9γ given in the text of their 1965 paper to -12γ for the reason stated in their "Note added in proof".] The estimate made by Akasofu et al. (1962), based on an earlier version of the Explorer 12 results gave a decrease of -38γ at the earth's surface and a minimum of -72γ at 4.1 R_e. It has already been discussed in an earlier section that apart from the magnitude of the field depression, its dependence on radial distance derived from these model calculations does not agree with the observational results presented in this paper.

With the Explorer 26 magnetometer Cahill (1966) was able to study the storm-time ring current. He observed that the greatest field depression at the maximum main phase of the storm of April 17, 1965 was near 3 R_e. It is interesting to note that except for the different degrees of severity the inflation of the inner magnetosphere shown in this paper for quiet or only slightly disturbed periods is not dissimilar to that for a storm time studied by Cahill.

(iii) Asymmetry with Respect to the Equator

The ΔB contours for the nightside magnetosphere presented in Figure 1 show conspicuous asymmetry with respect to the dipole equator. To examine if this is a seasonal effect, due to the variation in the sun's declination and hence the solar wind direction, the following procedure was taken. To each data point used to determine the average ΔB contours, a season number was assigned. Season numbers are: 1.0 for the winter months, November, December, January, and February, 2.0 for the equinoctial months, March, April, September, and October, and 3.0 for the summer months, May, June, July, and August. For each volume element in which ΔB values were averaged, the season numbers were also averaged to obtain the mean season number to be associated with the mean ΔB for the volume element. In the nightside equatorial region the mean season number was then found to be very close to the summer value of 3.0 at all distances $\geq 2\ R_e$. To give a quantitative result, the overall average season number for the region between 2 and 12 R_e and within dipole latitudes $\pm 15^o$ was 2.91, meaning that the ΔB contours in this region represent a summer condition. We consider this to be the cause for the inclination of the ΔB contours toward the southern hemisphere in the nightside equatorial magnetosphere seen in Figure 1. No other sectors shown in Figures 1 to 4 have enough coverage of data to meaningfully investigate such a seasonal effect, but the midnight sector in Figure 3 for Kp = 2-3 shows some indication of a similar seasonal effect. Use of other coordinate systems that incorporate the variation of the sun's declination, such as solar magnetospheric coordinates, will be an obvious future extension of the present study.

CONCLUSIONS

The rubidium magnetometer observations on OGO's 3 and 5 have provided extensive scalar field data to investigate the distortions of the magnetospheric field. Maps of average equal ΔB contours derived from these data for the geomagnetic noon-midnight and dawn-dusk meridian planes show two significant features: (a) high latitude $+\Delta B$ regions in the nightside magnetosphere, and (b) an equatorial $-\Delta B$ region in the inner magnetosphere.

(a) The high latitude $+\Delta B$ regions. Although the observation of a $+\Delta B$ region is presented in this paper for northern high latitudes, it is tacitly assumed that a similar region exists at corresponding southern latitudes. The available data for the southern hemisphere, though not extending to as high latitudes as in the northern hemisphere, indicate nothing suggesting existence of major north-south asymmetry in this regard. Near midnight ΔB increases toward the polar magnetosphere, and the maximum ΔB exceeds 50γ at 55 to 60° dipole latitude and at distances 6 to 8 R_e when Kp = 2-3. Such high fields cannot be explained by the existing theoretical models of the magnetosphere.

(b) The equatorial $-\Delta B$ region. Its existence implies large inflation of the inner magnetosphere even under magnetically quiet conditions. The minimum ΔB is $< -50\gamma$ for Kp = 2-3. The observed distribution of ΔB as a function of radial distance is quite different from that of the quiet-time ring current models of the type generally calculated (e.g., Akasofu et al., 1962; Hoffman and Bracken, 1965, 1967). The observations indicate that ΔB decreases toward the earth to distances $\lesssim 3$ R_e even at quiet times. The "disk-shaped" quiet-time ring current envisioned on the basis of the present magnetic observations differs substantially from the quiet-time ring current described as such by Frank (1967, 1970, 1971) based on his observation of low-energy protons which during quiet-times were centered at about 6.5 R_e. Our observations show that the ring current intensity varies with magnetic activity even at the lowest levels of Kp. The storm-time ring current can thus be viewed as an intensification of the quiet-time ring current.

For future observational programs it is highly desirable: (a) to survey the magnetic field in the polar magnetosphere and in near earth regions at distances $\lesssim 3\ R_e$ (where there is a gap between the altitudes covered by the POGO satellites and those regions studied in this paper), and (b) to measure low-energy particles in the equatorial region at distances of 1.5 to 5 R_e.

Acknowledgement. We wish to express our gratitude to Dr. R. A. Hoffman and F. W. Berko for providing numerical results for the quiet-time ring current model.

REFERENCES

Akasofu, S.-I., J. C. Cain, and S. Chapman, The magnetic field of the quiet-time proton belt, _J. Geophys. Res._, _67_, 2645, 1962.

Benkova, N. P., and S. Sh. Dolginov, The survey with Cosmos-49, in _The World Magnetic Survey 1957-1969_, IAGA Bulletin No. 28, International Association of Geomagnetism and Aeronomy, edited by A. J. Zmuda, IUGG Publications Office, Paris, 1971 (in press).

Cahill, L. J., Jr., Inflation of the inner magnetosphere during a magnetic storm, _J. Geophys. Res._, _71_, 4505, 1966.

Cahill, L. J., Jr., Magnetosphere inflation during four magnetic storms in 1965, _J. Geophys. Res._, _75_, 3778, 1970.

Cain, J. C., and R. A. Langel, Geomagnetic survey by the Polar Orbiting Geophysical Observatories, in _The World Magnetic Survey 1957-1969_, IAGA Bulletin No. 28, International Association of Geomagnetism and Aeronomy, edited by A. J. Zmuda, IUGG Publications Office, Paris, 1971 (in press).

Cain, J. C., S. J. Hendricks, R. A. Langel, and W. V. Hudson, A proposed model for the International Geomagnetic Reference Field - 1965, _J. Geomag. Geoelec._, _19_, 335, 1967.

Cummings, W. D., and P. J. Coleman, Jr., Simultaneous magnetic field variations at the earth's surface and at synchronous, equatorial distance. Part I. Bay-associated events, _Radio Sci._, _3_, 758, 1968.

Cummings, W. D., J. N. Barfield, and P. J. Coleman, Jr., Magnetospheric substorms observed at the synchronous orbit, _J. Geophys. Res._, _73_, 6687, 1968.

Davis, L. R., and J. M. Williamson, Low-energy trapped protons, _Space Res._, _3_, 365, 1963.

Fairfield, D. H., Average magnetic field configuration of the outer magnetosphere, _J. Geophys. Res._, _73_, 7329, 1968.

Fairfield, D. H., The configuration of the geomagnetic field, preprint, Goddard Space Flight Center, X-692-70-163, 1970.

Frank, L. A., On the extraterrestrial ring current during geomagnetic storms, _J. Geophys. Res._, _72_, 3753, 1967.

Frank, L. A., Direct detection of asymmetric increases of extraterrestrial 'ring current' proton intensities in the outer radiation zone, _J. Geophys. Res._, _75_, 1263, 1970.

Frank, L. A., Relationship of the plasma sheet, ring current, trapping boundary, and plasmapause near the magnetic equator and local midnight, _J. Geophys. Res._, _76_, 2265, 1971.

Frank, L. A., and H. D. Owens, Omnidirectional intensity contours of low-energy protons ($0.5 \le E \le 50$ kev) in the earth's outer radiation zone at the magnetic equator, _J. Geophys. Res._, _75_, 1269, 1970.

Heppner, J. P., Recent measurements of the magnetic field in the outer magnetosphere and boundary regions, _Space Sci. Rev._, _7_, 166, 1967a.

Heppner, J. P., Satellite and rocket observations, in _Physics of Geomagnetic Phenomena_, edited by S. Matsushita and W. H. Campbell, pp. 935-1036, Academic Press, New York, 1967b.

Heppner, J. P., M. Sugiura, T. L. Skillman, B. G. Ledley, and M. Campbell, OGO-A magnetic field observations, _J. Geophys. Res._, _72_, 5417, 1967.

Hoffman, R. A., and P. A. Bracken, Magnetic effects of the quiet-time proton belt, _J. Geophys. Res._, _70_, 3541, 1965.

Hoffman, R. A., and P. A. Bracken, Higher-order ring currents and particle energy storage in the magnetosphere, _J. Geophys. Res._, _72_, 6039, 1967.

Jensen, D. C., and J. C. Cain, An interim geomagnetic field (Abstract), J. Geophys. Res., 67, 3568, 1962.

Ledley, B. G., Magnetometers for space measurements over a wide range of field intensities, Rev. d. Phys. Appl. 5, 164, 1970.

Ness, N. F., Observations of the interaction of the solar wind with the geomagnetic field during quiet conditions, in Solar-Terrestrial Physics, edited by J. W. King and W. S. Newman, pp. 57-89, 1967.

Ness, N. F., The geomagnetic tail, Rev. Geophys., 7, 97, 1969.

Olson, W. P., and W. D. Cummings, Comparison of the predicted and observed magnetic field at ATS 1, J. Geophys. Res., 75, 7117, 1970.

Skillman, T. L., ATS-E magnetic field monitor instrumentation, Rep. X-645-70-54, Goddard Space Flight Center, 1970.

Sugiura, M., Results of magnetic surveys of the magnetosphere and adjacent regions, in The World Magnetic Survey 1957-1969, IAGA Bulletin No. 28, International Association of Geomagnetism and Aeronomy, edited by A. J. Zmuda, IUGG Publications Office, Paris, 1971 (in press).

Sugiura, M., T. L. Skillman, B. G. Ledley, and J. P. Heppner, Magnetic field observations in high β regions of the magnetosphere, in Particles and Fields in the Magnetosphere, edited by B. M. McCormac, pp. 165-170, D. Reidel Publishing Company, Dordrecht, Holland, 1970.

Williams, D. J., and G. D. Mead, Nightside magnetosphere configuration as obtained from trapped electrons at 1100 kilometers, J. Geophys. Res., 70, 3017, 1965.

Zmuda, A. J., 1964 83C, in The World Magnetic Survey 1957-1969, IAGA Bulletin No. 28, International Association of Geomagnetism and Aeronomy, edited by J. A. Zmuda, IUGG Publications Office, Paris, 1971 (in press).

TITLES OF FIGURES

Figure 1 : Contours of equal ΔB in the geomagnetic noon-midnight meridian plane for a quiet condition, Kp = 0-1; units: gamma.

Figure 2 : Contours of equal ΔB in the geomagnetic dawn-dusk meridian plane for a quiet condition, Kp = 0-1; units: gamma.

Figure 3 : Contours of equal ΔB in the geomagnetic noon-midnight meridian plane for a slightly disturbed condition, Kp = 2-3; units: gamma.

Figure 4 : Contours of equal ΔB in the geomagnetic dawn-dusk meridian plane for a slightly disturbed condition, Kp = 2-3; units: gamma.

Figure 5 : Contours of equal ΔB in the noon-midnight meridian plane for the Mead-Williams model with a high tail field; unit: gamma.

Figure 6 : Contours of equal ΔB for the noon meridian based on a quiet time ring current model developed by Hoffman and Bracken.

Figure 7 : ΔB on the dipole equatorial plane as a function of radial distance: for the Hoffman-Bracken quiet-time ring current model (at noon) and for observed ΔB for noon and midnight.

Figure 8 : ΔB plotted against dipole latitude for the 90 degree sector centered at geomagnetic midnight and between 4 and 6 R_e. On each orbit, intervals between data points are ≥ 1 R_e so that the maximum number of data points contributing to this plot from any one orbit is two.

Figure 9 : ΔB plotted against dipole latitude for the 90 degree sector centered at geomagnetic midnight and between 6 and 8 R_e. The remark made in the caption for Figure 8 also applies.

Figure 10: Relation between equatorial crossing distances of field lines and dipole latitudes of their feet on the earth's surface in the geomagnetic noon-midnight meridian plane. Note the change in the vertical scale at 60 degrees.

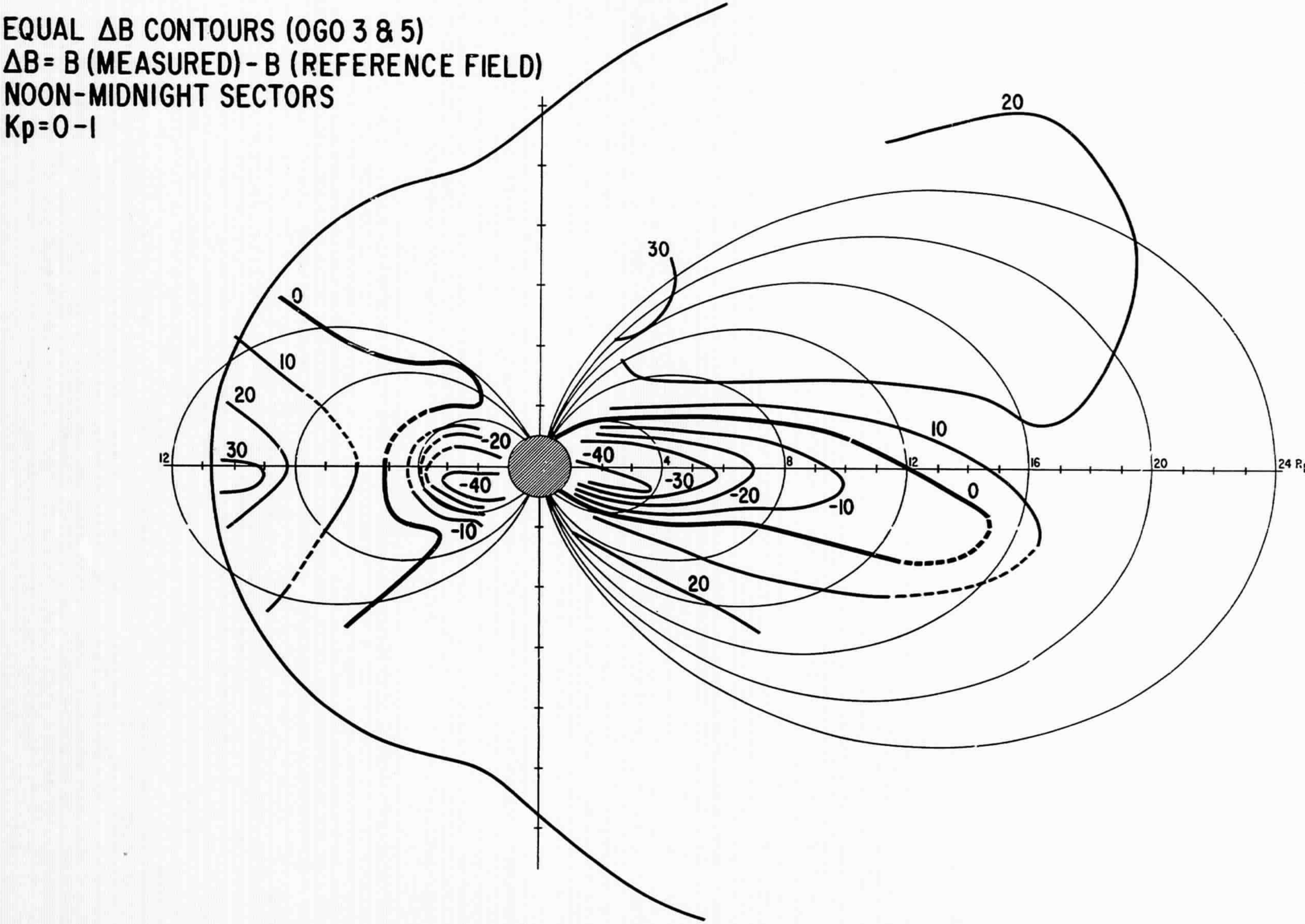

EQUAL ΔB CONTOURS (OGO 3 & 5)
ΔB = B (MEASURED) - B (REFERENCE FIELD)
NOON-MIDNIGHT SECTORS
Kp=0-1
20
30
0
10
20
30
-20
-40
-10
-40
-30
-20
-10
10
0
20
12
4
8
12
16
20
24 R_E

FIGURE 1

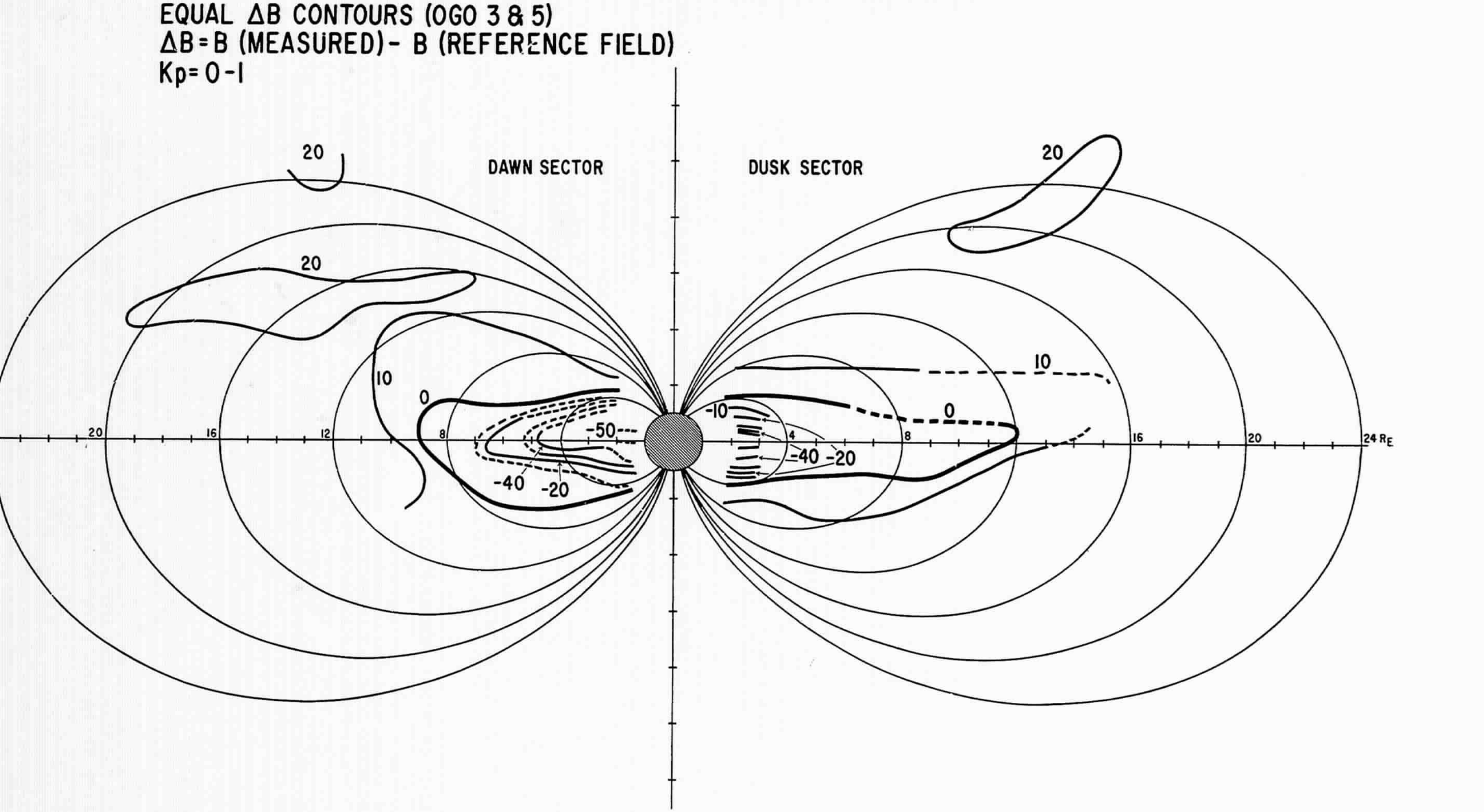

EQUAL ΔB CONTOURS (OGO 3 & 5)
ΔB = B (MEASURED) - B (REFERENCE FIELD)
Kp = 0-1
DAWN SECTOR
DUSK SECTOR
20
20
20
10
10
0
0
-10
-50
-40
-20
-40
-20
4
8
12
16
20
24 RE

FIGURE 2

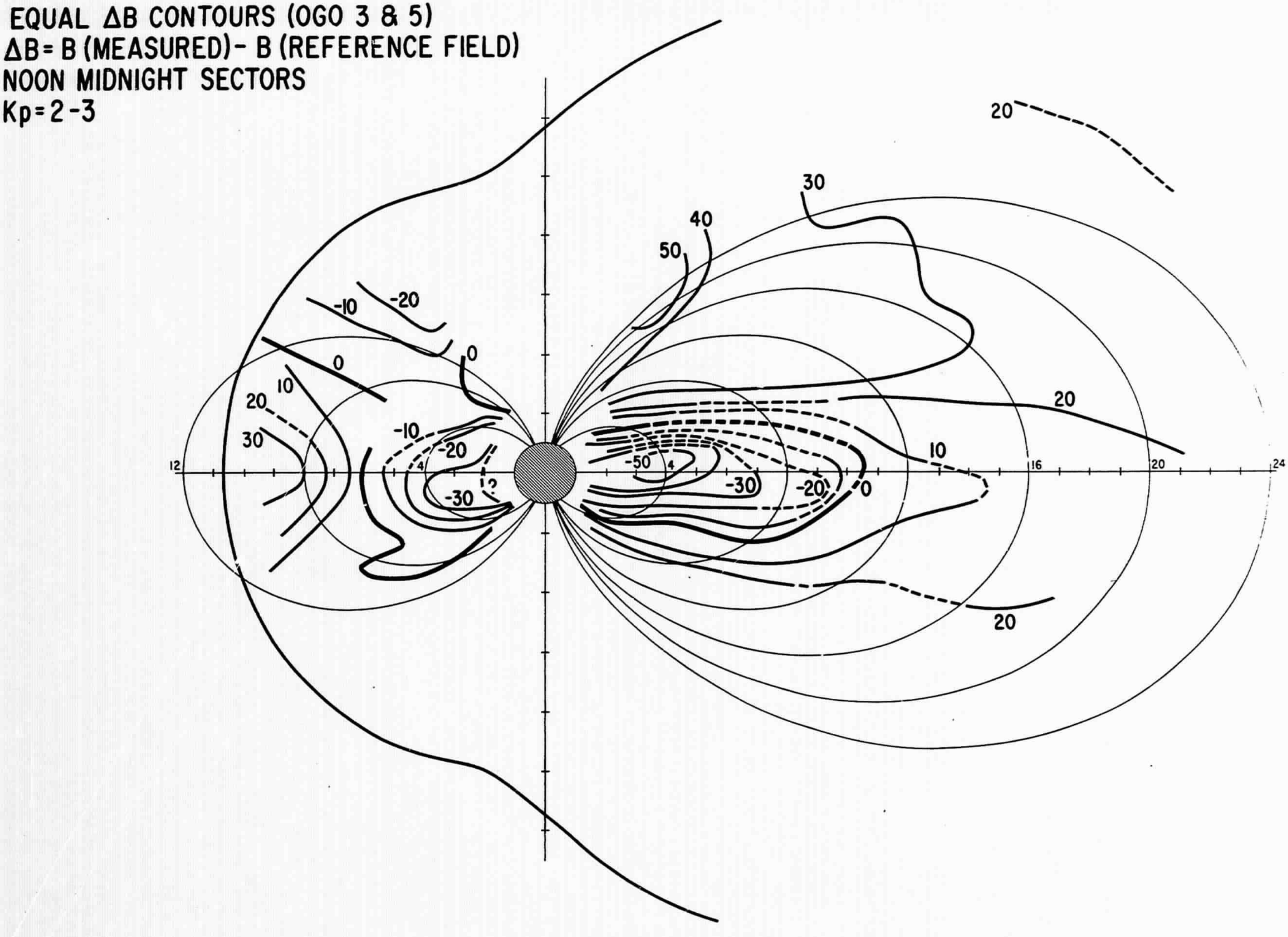
EQUAL ΔB CONTOURS (OGO 3 & 5)
ΔB= B (MEASURED)- B (REFERENCE FIELD)
NOON MIDNIGHT SECTORS
Kp=2-3
12
16
20
24
30
40
50
20
10
0
-10
-20
-30
-50
4

FIGURE 3

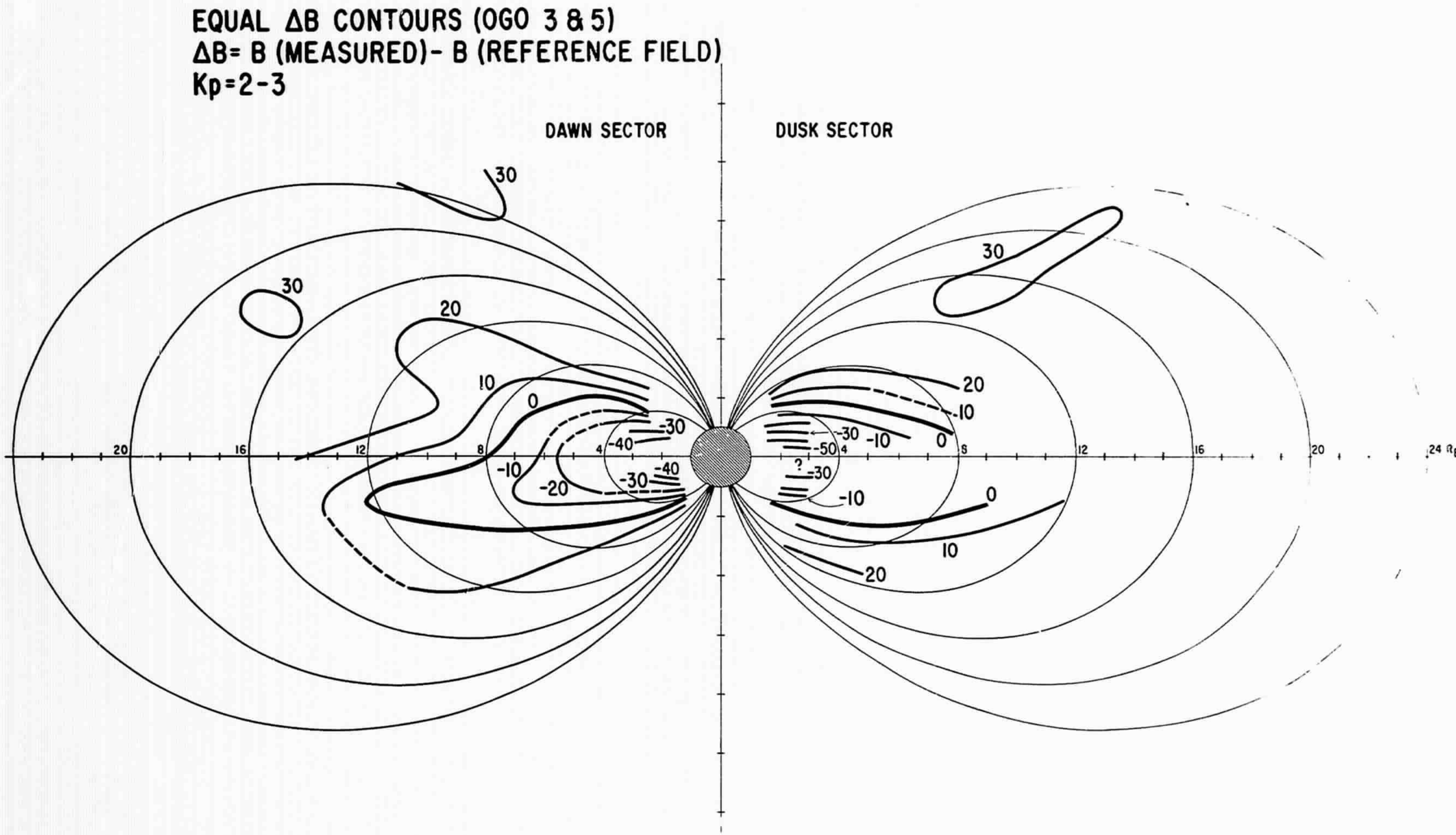
EQUAL ΔB CONTOURS (OGO 3 & 5)
ΔB= B (MEASURED) - B (REFERENCE FIELD)
Kp=2-3
DAWN SECTOR
DUSK SECTOR
24 R_E

FIGURE 4

EQUAL ΔB CONTOURS FOR
MEAD-WILLIAMS MODEL
NOON-MIDNIGHT MERIDIAN
(HIGH TAIL FIELD)

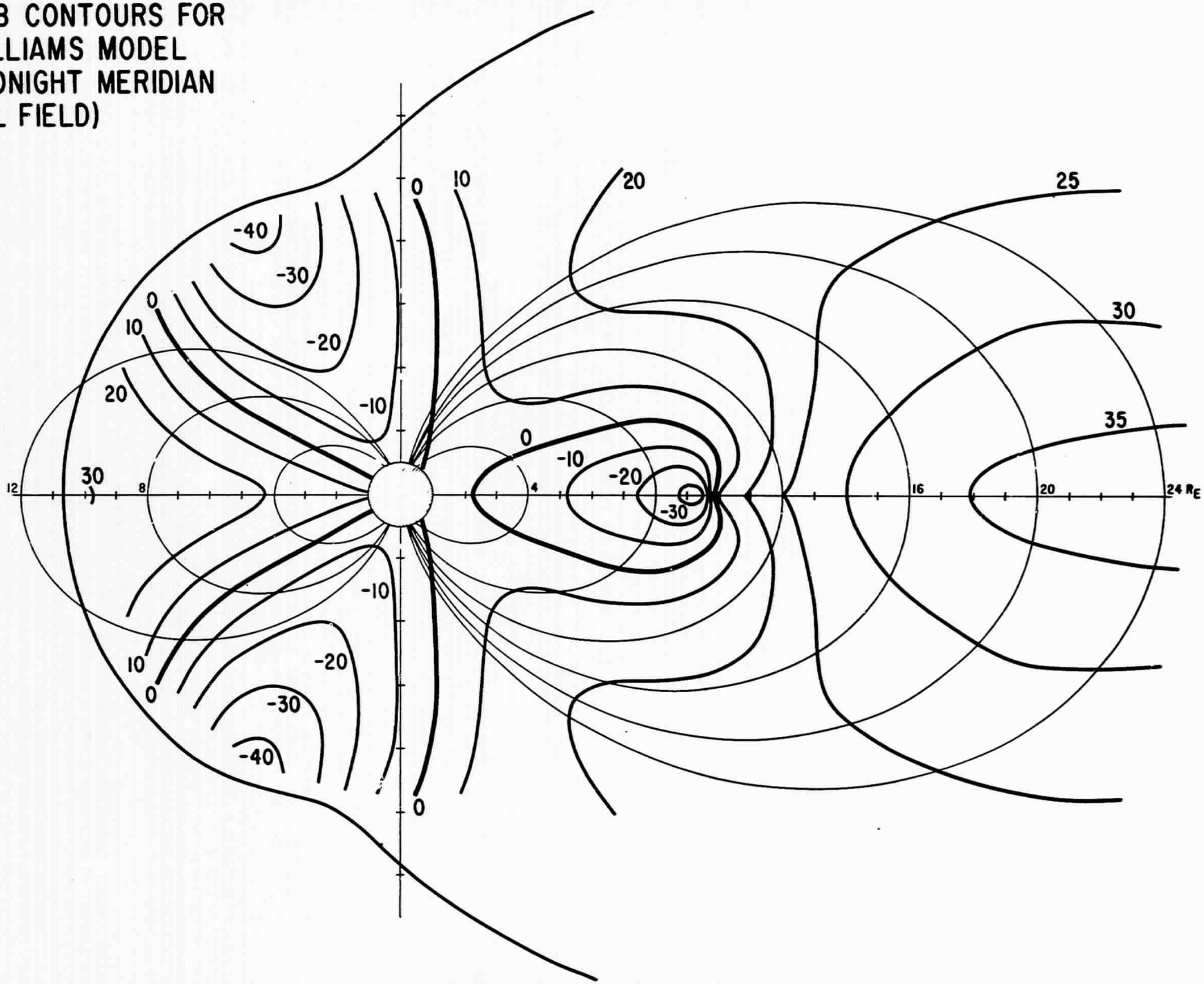

FIGURE 5

EQUAL ΔB CONTOURS FOR HOFFMAN-BRACKEN QUIETTIME RING CURRENT MODEL (UNIT: GAMMA)

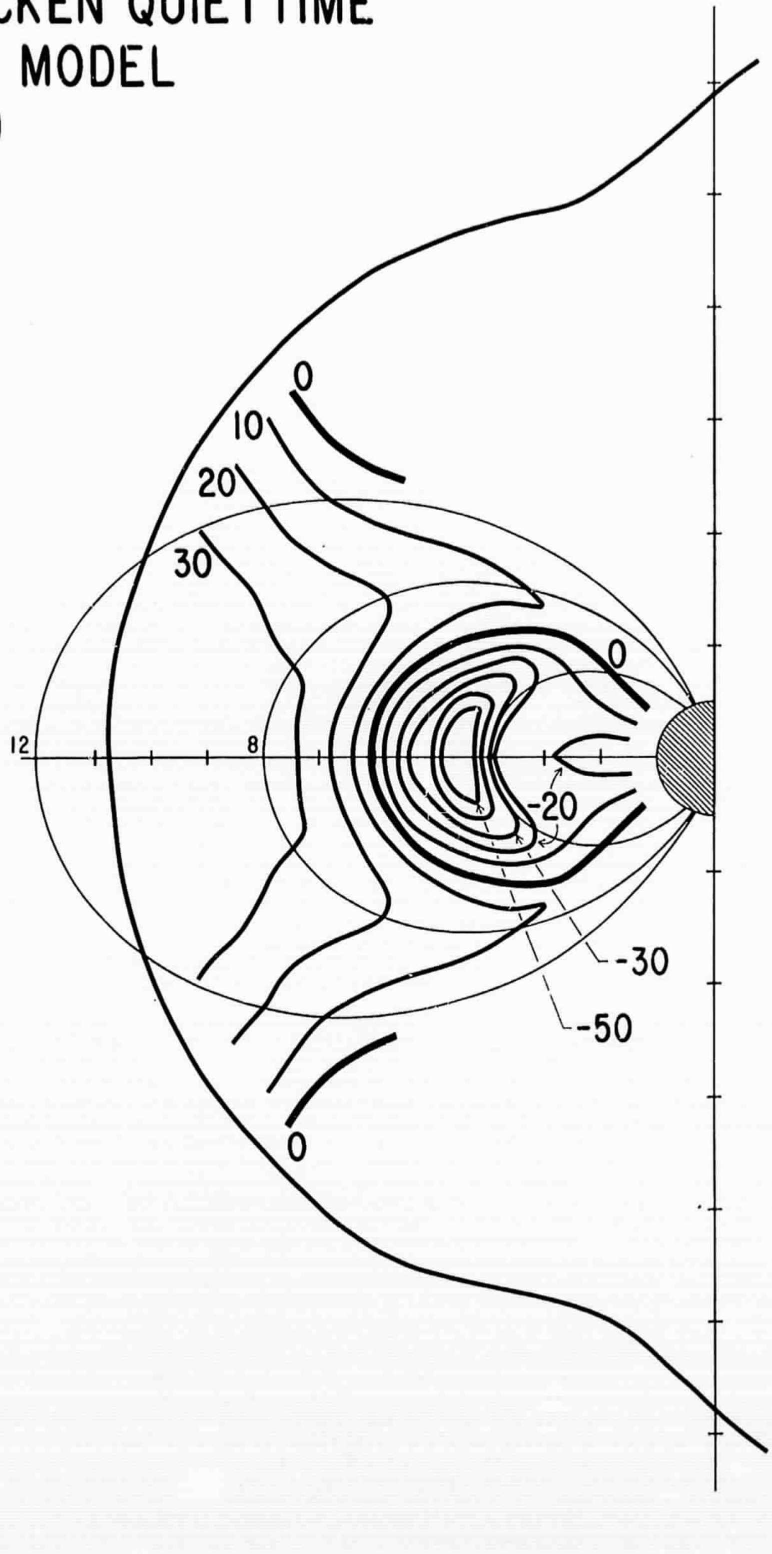

FIGURE 6

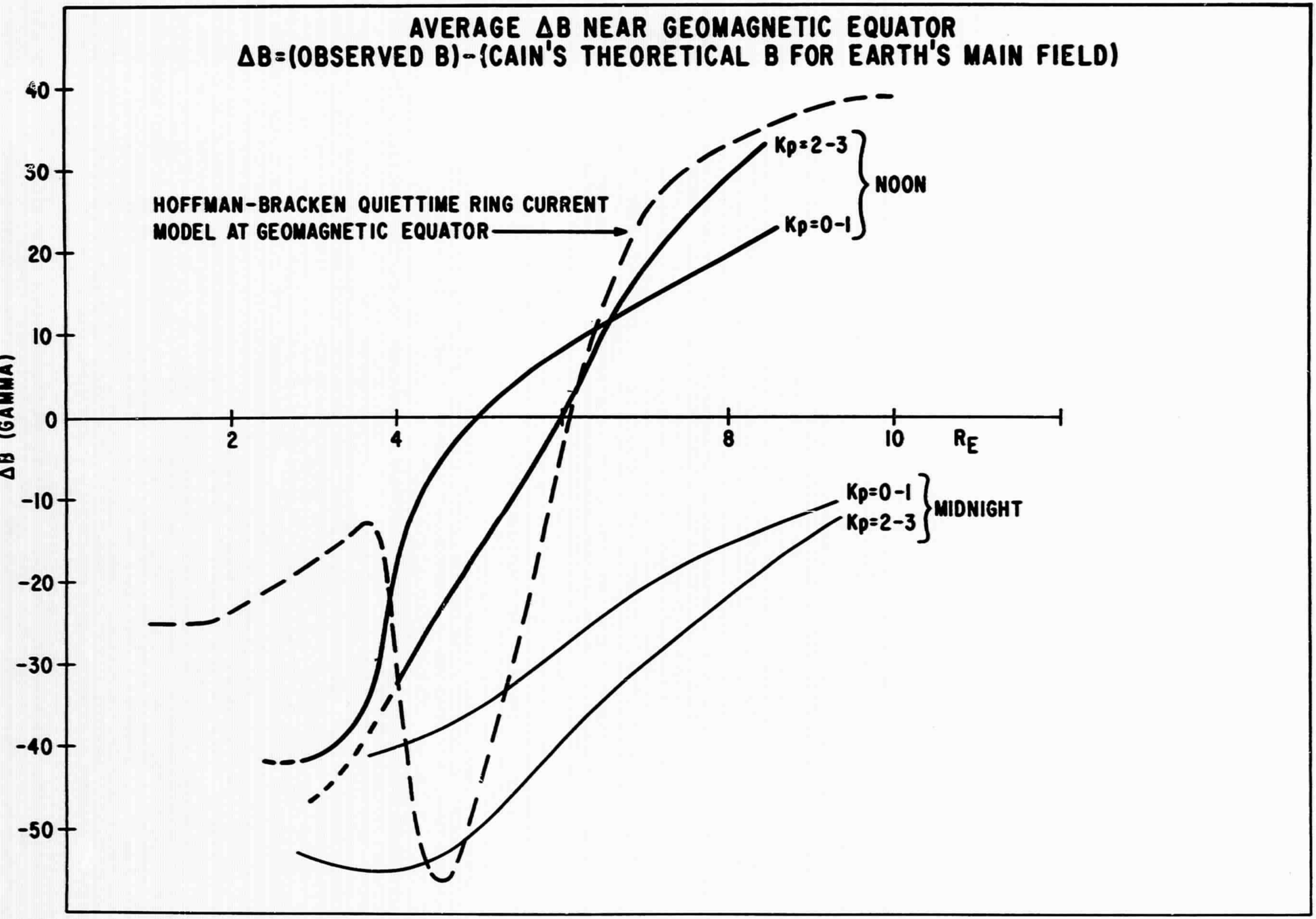
AVERAGE ΔB NEAR GEOMAGNETIC EQUATOR
ΔB=(OBSERVED B)-(CAIN'S THEORETICAL B FOR EARTH'S MAIN FIELD)
HOFFMAN-BRACKEN QUIETTIME RING CURRENT
MODEL AT GEOMAGNETIC EQUATOR
Kp=2-3
Kp=0-1
NOON
Kp=0-1
Kp=2-3
MIDNIGHT
ΔB (GAMMA)
40
30
20
10
0
-10
-20
-30
-40
-50
2
4
8
10
R_E

FIGURE 7

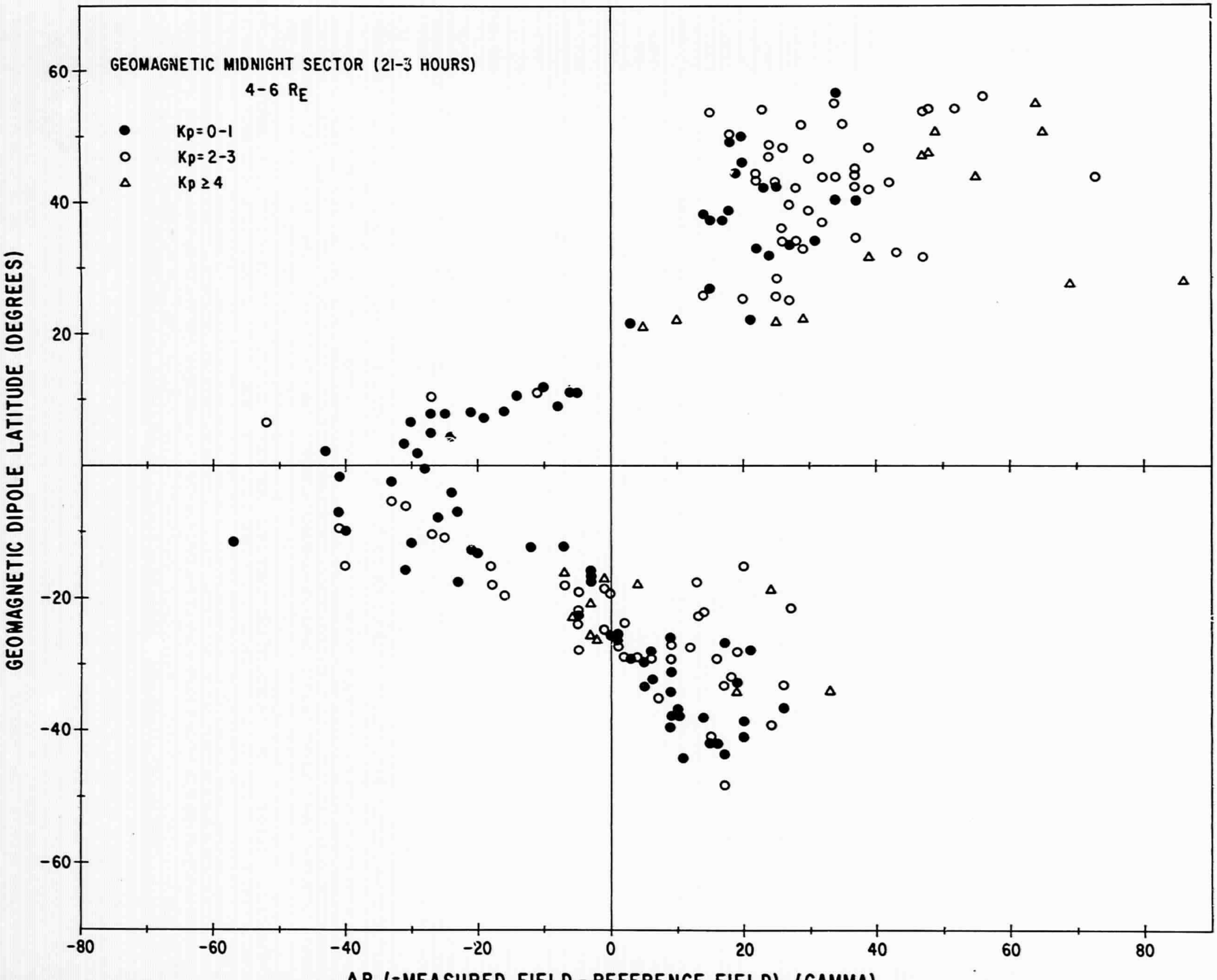
GEOMAGNETIC MIDNIGHT SECTOR (21-3 HOURS)
4-6 R_E
Kp=0-1
Kp=2-3
Kp ≥ 4
GEOMAGNETIC DIPOLE LATITUDE (DEGREES)
60
40
20
-20
-40
-60
-80
-60
-40
-20
0
20
40
60
80
ΔB (=MEASURED FIELD - REFERENCE FIELD) (GAMMA)

FIGURE 8

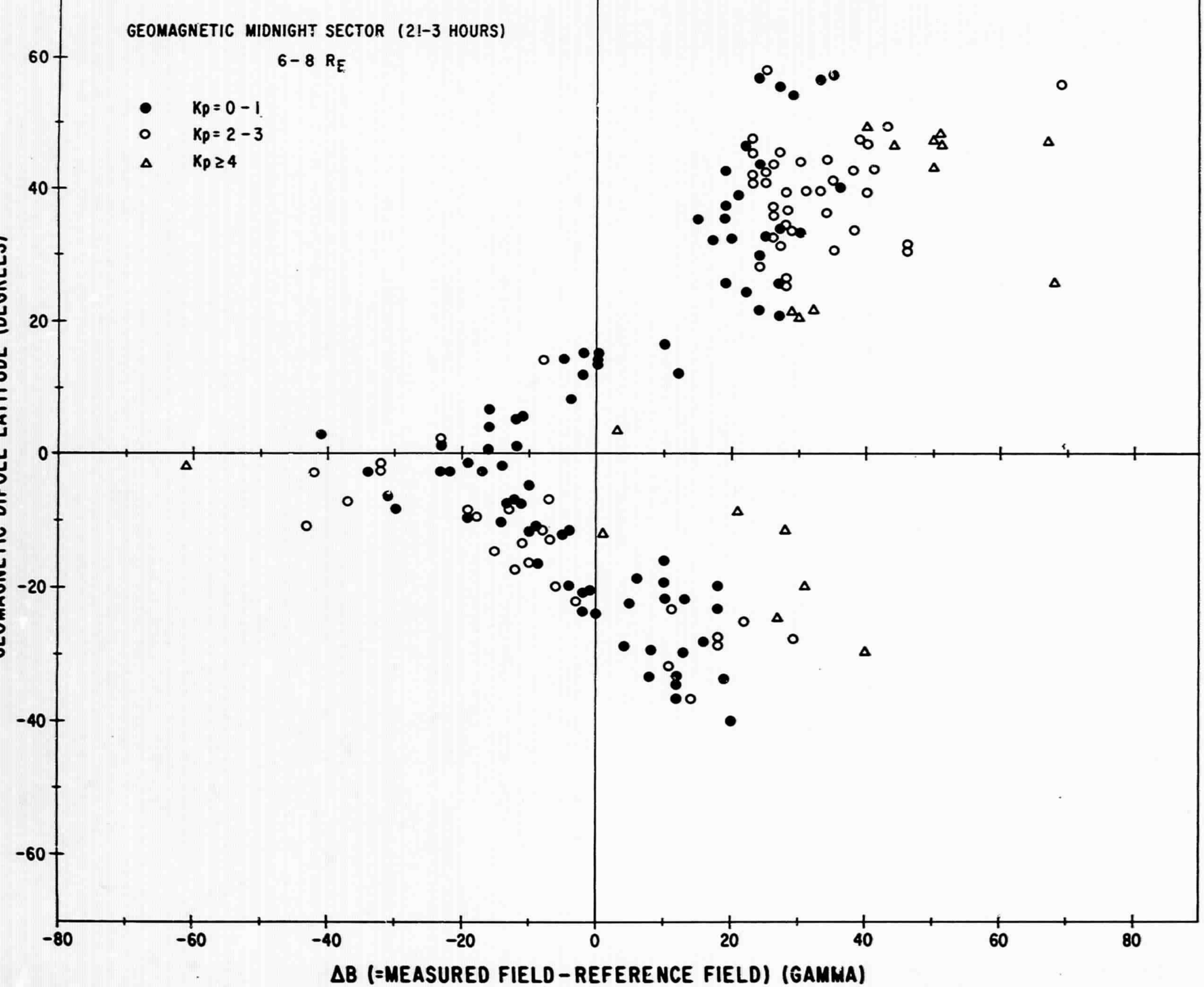

GEOMAGNETIC MIDNIGHT SECTOR (21-3 HOURS)
6-8 R_E
Kp = 0 - 1
Kp = 2 - 3
Kp ≥ 4
60
40
20
0
-20
-40
-60
-80
-60
-40
-20
0
20
40
60
80
ΔB (=MEASURED FIELD-REFERENCE FIELD) (GAMMA)

FIGURE 9

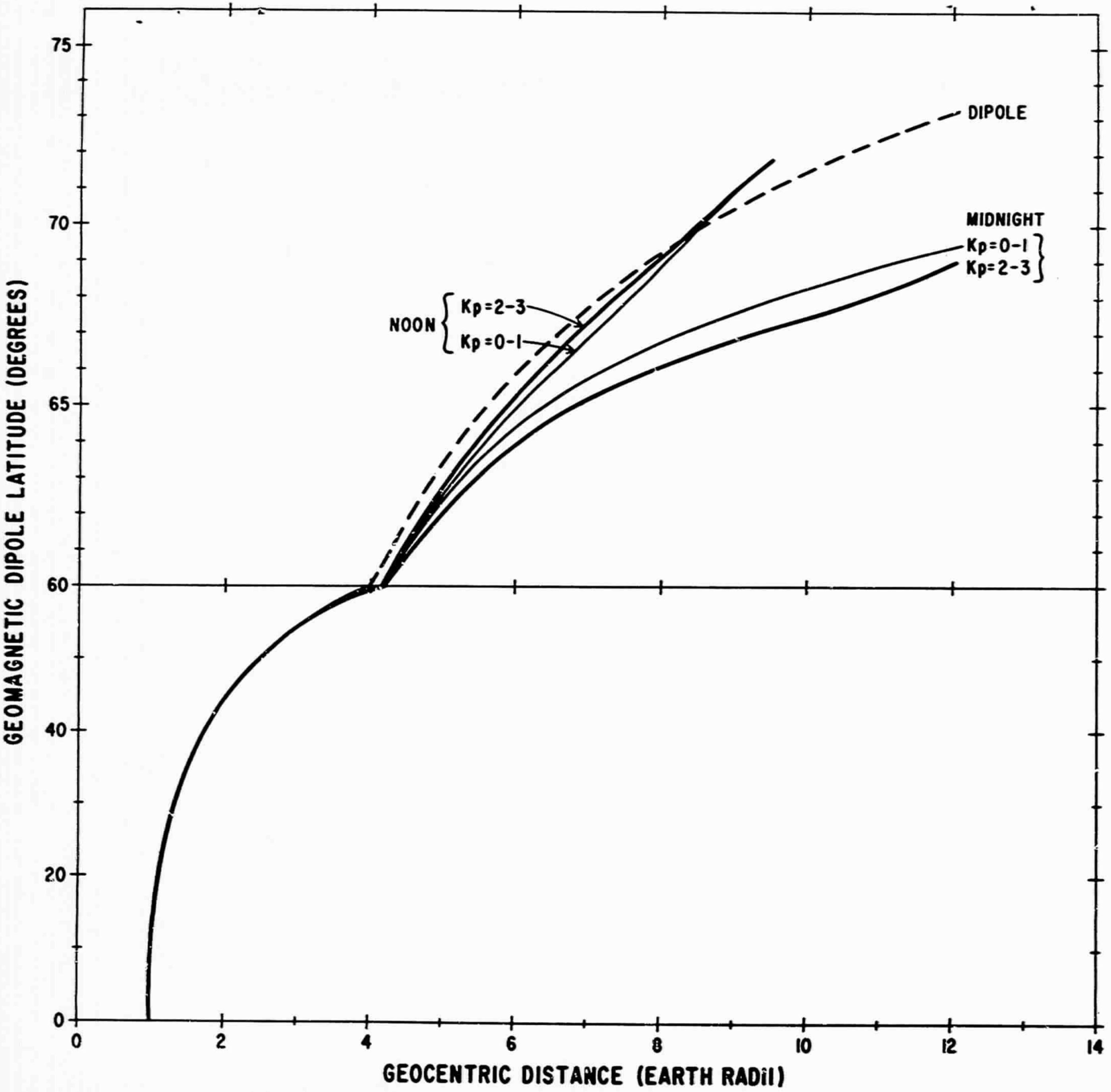

DIPOLE
MIDNIGHT
Kp=0-1
Kp=2-3
NOON
Kp=2-3
Kp=0-1
75
70
65
60
40
20
0
0
2
4
6
8
10
12
14
GEOMAGNETIC DIPOLE LATITUDE (DEGREES)
GEOCENTRIC DISTANCE (EARTH RADII)

FIGURE 10